nature portfolio

https://doi.org/10.1038/s41587-021-00878-8

Supplementary information

Engineering luminescent biosensors for point-of-care SARS-CoV-2 antibody detection

In the format provided by the authors and unedited

Supplementary Text:

S sensor engineering and characterization

Linker modeling

We modeled S-RBD binding to two antibodies to determine the optimal linker lengths between the S-RBD domains and the SmBiT/LgBiT fusions. The antibody C105 is an ACE2-competitive binder (**Extended Data Fig. 1c**)[1,2], while the antibody CR3022 does not compete with ACE2 (**Extended Data Fig. 1d**)[3]. Based on the assumption that the wing-span of antigen binding sites between Fab arms on a flexible-hinge region of an Fc are roughly ~117-134 Å apart[4], and residue-to-residue distance in a linker lies between the length of tightly packed alpha-helix residues (1.5 Å) and extended beta-strand residues (3.5 Å), we estimated the total number of linker residues should be ~30-80 amino acids. Antibodies binding to the CR3022 epitope may require a shorter linker for NanoLuc reconstitution (**Extended Data Fig. 1d**) than antibodies competitive with ACE2 (**Extended Data Fig. 1c**). Considering S-RBD has a C-terminal 15-residue loop to function as part of the linker, we constructed SmBiT fusions to S-RBD C-terminus with 15 or 25 residue Glycine/Serine (GS) linkers (S15 and S25), and LgBiT fusions to S-RBD C-terminus with 5, 15, or 25 residue GS linkers (L5, L15 and L25). These linker variants were expressed in Expi293 cells and varied in expression yields (**Extended Data Fig. 1e**). The N-terminal fusions to S-RBD were not designed because the N and C termini localize in close proximity and we hypothesized this alternative fusion design would result in similar sensor performance as the C-terminal fusions (**Extended Data Fig. 1b**). All modeling was performed in PyMoL.

Optimization of enzyme concentrations, linkers and buffer conditions

We then determined the optimal enzyme concentration. A three-fold dilution series from 27 to 0.11 nM of the L15 + S25 sensors were mixed with increasing 10-fold dilutions of recombinant CR3022 (**Extended Data Fig. 1f**). After a 20-minute incubation, the NanoLuc substrate was added and allowed to develop for 10 minutes before luminescence signal was read. High sensor concentrations (27, 9, 3 nM) resulted in stronger background luminescence signal and therefore lower detection sensitivity of CR3022, due to increased basal association of the two split sensors. Meanwhile, low sensor concentrations (0.33 and 0.1 nM) generated overall less signal than 1 nM sensors because fewer sensors are captured on each antibody. As a result, sensors at 1 nM were used in all subsequent assays.

Next, we queried if linker lengths affect detection sensitivity. Sensors with varied linker lengths were mixed with 10-fold dilutions of CR3022 and all resulted in dose-dependent luminescence signals (**Extended Data Fig. 1f**). Little difference in detection sensitivity was observed, except that the (L5 + S15) and (L5 + S25) linker combinations resulted in slightly decreased sensitivity at low antibody concentrations. This result indicated that we had selected a proper range of linker lengths. Based on robust signal and expression yields (**Extended Data Fig. 1e**), we chose the L15 and S25 sensor pair for subsequent assays.

Interestingly, we observed that the regular PBSTB assay buffer (PBS, 0.05% Tween-20, 0.2% m/v BSA, PBSTB) produced a higher background signal (average relative luciferase units (RLU) = 70-80) than in serum samples (RLU = 24.5). We tested if supplementing Fetal Bovine Serum (FBS) can reduce background (**Supplementary Fig. 1**). PBS + 0.05% Tween-20 (PBST) with 4-10 % FBS was found to reduce the signal (mean RLU = 21) to a level that is close to signal from 12.5% serum, and therefore can serve as a proper negative control. Both the recombinant anti-S antibody C004 and the commercial anti-N antibody (Sino biological, Cat#40588-T62-50)

produced linear dose-dependent signal in this buffer (**Fig. 1b and c**), which can be used to generate standard curves and calibrate the instruments for the spLUC assay.

Impact of binding affinities

To determine whether the affinity of the target binding to S-RBD affects signal strength, we turned to two dimeric ACE2 constructs: ACE2-Fc, which is the human ACE2 peptidase domain fused to IgG1 Fc[5], and an engineered ACE2-Fc variant that binds ~10x tighter to S-RBD (**Extended Data Fig. 2**). Overall, signal from wild-type ACE2-Fc (K_D = 10 nM) is weak, with signal that is more than two standard deviations above background only detected at the highest tested ACE2-Fc concentration (10 nM). Conversely, the enhanced-affinity ACE2-Fc variant (K_D = 1 nM) generated a dose-dependent signal from 0.1-10 nM protein concentrations and exhibited 2.6-fold higher signal observed at 10 nM relative to the wild-type ACE2-Fc. These findings indicated the sensors report the presence of not only larger quantities of anti-S-RBD binders but also higher-affinity binders. This property of the sensors suggested spLUC assay may be used to characterize binding affinities of S-RBD antibodies or ACE2 variants for therapeutic applications.

Thermodynamic sensor model

In further characterizing the relationship between assay signal strength and antibody concentration/binding affinity, we performed ordinary differential equation modeling in R. We made assumptions such as a sensor can only be bound by one antibody, that antibody binding is non-cooperative, and that there is no detectable basal affinity of LgBiT and SmBiT at the concentrations tested (**Extended Data Fig. 3a**). The modeling predicted a linear relationship

between antibody concentration and luciferase signal (**Extended Data Fig. 3b**), consistent with our experimental data (**Fig. 1b, c**).

The following set of ordinary differential equations (ODEs) was written to describe the system depicted in **Extended Data Fig. 3a** and generated the curve graphs in **Extended Data Fig. 3b and c**:

$$\frac{d[A]}{dt} = -k_{1f}[C][A] - k_{1f}[D][A] - k_{1f}[E][A] + k_{1r}[D] + k_{1r}[G] + k_{1r}[H]$$

$$\frac{d[B]}{dt} = -k_{1f}[C][B] - k_{1f}[E][B] - k_{1f}[D][B] + k_{1r}[E] + k_{1r}[I] + k_{1r}[H]$$

$$\frac{d[C]}{dt} = -k_{1f}[C][A] - k_{1f}[C][B] + k_{1r}[D] + k_{1r}[E]$$

$$\frac{d[D]}{dt} = -k_{1r}[D] - k_{1f}[D][A] - k_{1f}[D][B] + k_{1f}[C][A] + k_{1r}[G] + k_{1r}[H]$$

$$\frac{d[E]}{dt} = -k_{1r}[E] - k_{1f}[E][A] - k_{1f}[DE][B] + k_{1f}[C][B] + k_{1r}[H] + k_{1r}[I]$$

$$\frac{d[G]}{dt} = -k_{1r}[G] + k_{1f}[D][A]$$

$$\frac{d[H]}{dt} = -k_{1r}[H] - k_{1r}[H] + k_{1f}[D][B] + k_{1f}[E][A]$$

$$\frac{d[I]}{dt} = -k_{1r}[I] + k_{1f}[E][B]$$

Where:

A = LgBiT sensor

B = SmBiT sensor

C = Antibody

D = Antibody/ LgBiT sensor heterodimer

E = Antibody/ SmBiT sensor heterodimer

G = Antibody/ LgBiT sensor/LgBiT sensor trimer

H = Antibody/Active Enzyme trimer (Active Enzyme)

I = Antibody/ SmBiT sensor/SmBiT sensor trimer

k_{1f} = on rate of Antibody binding to Spike

k_{1r} = off rate of Antibody binding to Spike

For simplification, we assumed the following: 1) LgBiT sensor and SmBiT sensor had no measurable interaction, 2) Antibody binding to LgBiT sensor or SmBiT sensor was non-cooperative, and 3) Antibody binding to LgBiT sensor was equivalent in rate to antibody binding to SmBiT sensor. The equations above were solved in R using the deSolve package to find the concentration of each species at equilibrium. In all cases the initial concentrations of D,E,G,H, and I were set to 0. All thermodynamic modeling was performed in R, Rstudio and the deSolve package.

Supplementary Figures:

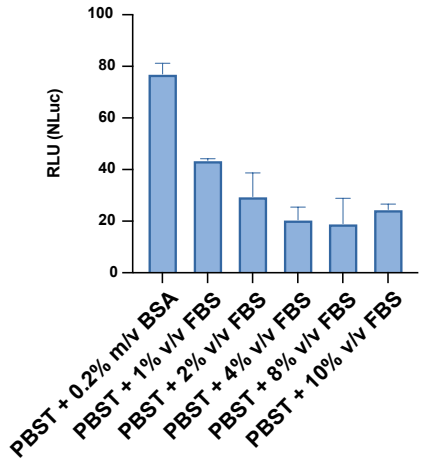

Supplementary Fig. 1 Supplementing FBS reduces background signal in spLUC assays. PBST with 4-10% FBS can be used as a negative control for serum samples as it shows similar signal suppression. Two technical replicates are plotted from n=1 individual experiment. Center of the bar represents the mean.

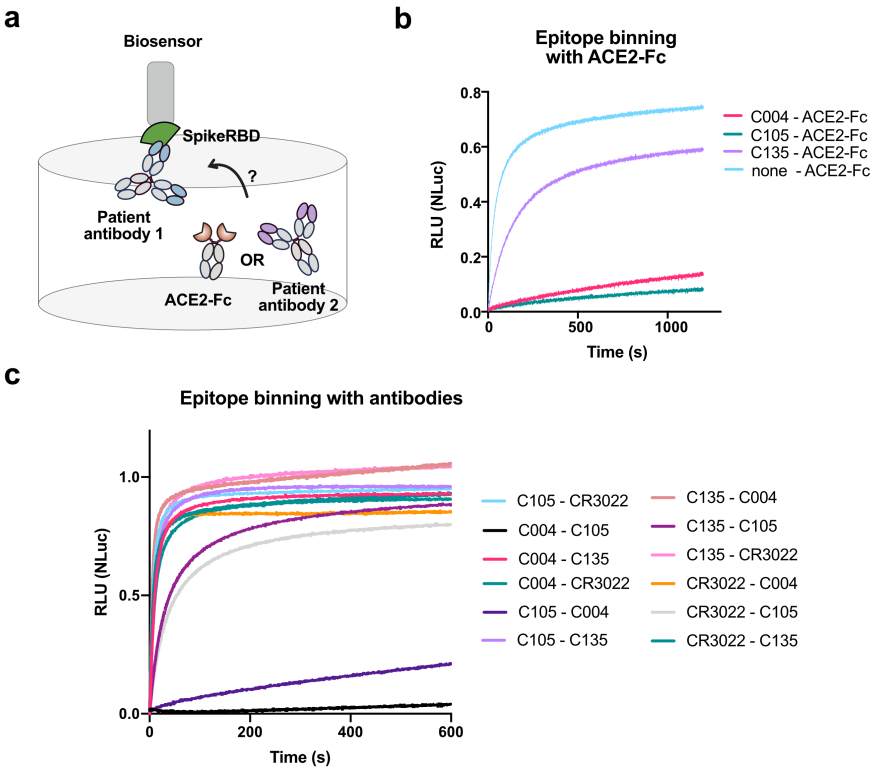

Supplementary Fig. 2 Epitope characterizations of CR3022, C004, C105 and C135. a, Design of a Biolayer interferometry (BLI) experiment to characterize competitive binding of the antibodies with ACE2-Fc and other antibodies. **b,** BLI experiments showed C004 and C105 both competed with ACE2-Fc for binding while C135 does not. **c,** BLI experiments showed C004 competed with C105 for binding while the other antibodies do not compete.

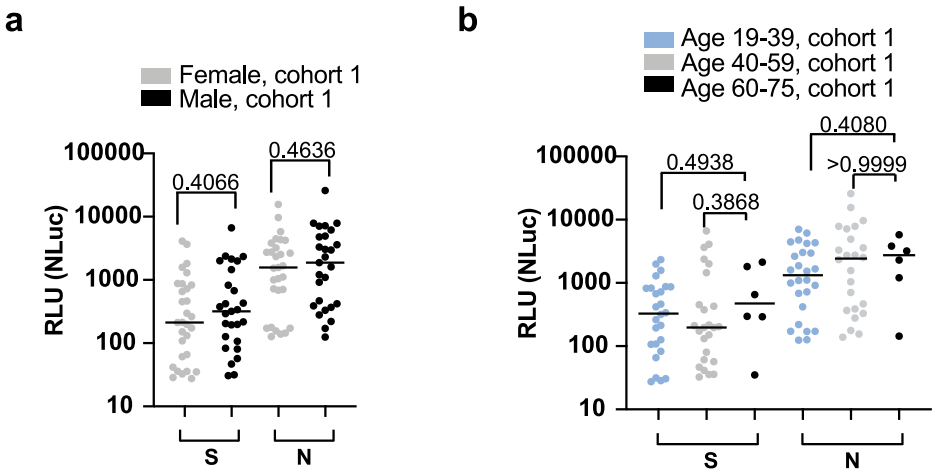

Supplementary Fig. 3 Further correlation of spLUC signal and gender/age. a, For cohort 1, males show a slightly higher spLUC assay signal compared to females, although this difference is not statistically significant. Samples sizes are as indicated in parentheses: S-female (30), S-male (27), N-female (29), and N-male (27). **b,** Cohort 1 spLUC signal shows no significant difference in signal among age groups. Samples sizes are as indicated in parentheses: age 19-39 (26), age 40-59 (24), and age 60-85 (6). For a and b, an unpaired Mann-Whitney test is performed and P values (two-tail) for each comparison are labeled on top of the datasets. Horizontal lines represent the median value. For both graphs, dots represent the average of two technical replicates from n=1 independent experiment.

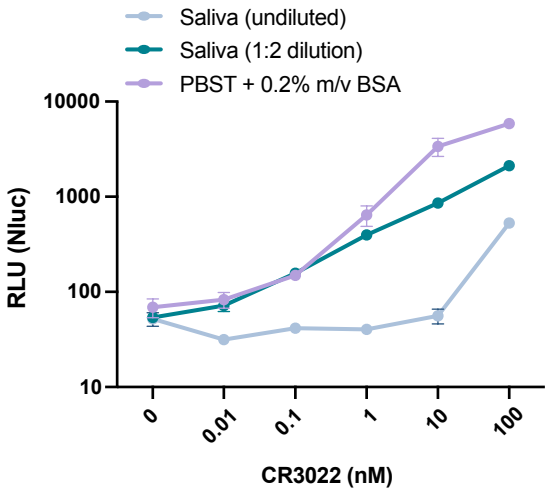

Supplementary Fig. 4 Saliva condition optimization. spLUC reactions are compatible with saliva samples. The CR3022 antibody was spiked into healthy individual saliva at 10-fold dilutions from 100 nM to 0.01 nM. While undiluted saliva reduced signal 10-fold and reduced sensitivity, 1:2 dilution of saliva only reduced signal by 3-fold and did not decrease the sensitivity. Two technical replicates are plotted from n=1 independent experiment. Lines connecting the means of the samples are plotted.

Supplementary Table. 1 Determination of assay cutoff values

	S	N
SERUM DILUTIONS	1:12.5	1:12.5
# SAMPLES	56	120
MIN	12	2.5
MAX	44.5	84
MEDIAN	23.2	25
MEAN	24.5	29.5
STANDARD DEVIATION (SD)	7.1	17.8
DERIVED CUTOFF (MEAN+3XSD)	45.9	83.1

Supplementary Table 2 A target profile proposed for SARS-CoV-2 serology tests in low resource areas

PROPERTY	OPTIMAL GOAL
SENSITIVITY	>95%
SPECIFICITY	>95%
QUANTIFICATION	Quantitative
SAMPLE TYPE	Whole blood, saliva
SAMPLE PROCESSING	Not required
REAGENT FORMAT	RT stable
TIME TO RESULT	< 30 min
DAILY THROUGHPUT	High
POWER REQUIREMENT	Battery
CONSUMABLE COST	< $10
DEVICE	Portable
MAINTENANCE	None
DATA ANALYSIS	Integrated

References and Notes

1. Robbiani, D. F. et al. Convergent antibody responses to SARS-CoV-2 in convalescent individuals. *Nature* **584**, 437–442 (2020).

2. Barnes, C. O. et al. Structures of human antibodies bound to SARS-CoV-2 spike reveal common epitopes and recurrent features of antibodies. *Cell* **182**, 828–842 (2020).

3. Yuan, M. et al. A highly conserved cryptic epitope in the receptor binding domains of SARS-CoV-2 and SARS-CoV. *Science* **368**, 630–633 (2020).

4. Sosnick, T. R. et al. Distances between the antigen-binding sites of three murine antibody subclasses measured using neutron and X-ray scattering. *Biochemistry* **31**, 1779-1786 (1992).

5. Glasgow, A. et al. Engineered ACE2 receptor traps potently neutralize SARS-CoV-2. *Proc. Natl. Acad. Sci. U.S.A.* **117**, 28046-28055 (2020).